A novel method to analyse MR pulmonary images based on the Phase-Resolved Functional Lung MRI (PREFUL) technique

Master Thesis

Cristina Crețu

August 2022

Faculty of Mechanical, Maritime and Materials Engineering (3mE)
Delft University of Technology

Abstract

Many pulmonary diseases, such as cystic fibrosis (CF), chronic obstructive pulmonary disease (COPD) or asthma are disrupting the lung perfusion/ventilation ratio. Therefore, monitoring it gives a good overview on the evolution of the disease. There are several imaging modalities to assess the ventilation and perfusion, but they either use ionizing radiation, are expensive, uncomfortable or pose the risk of allergic reactions. Fourier decomposition MRI is a radiation and contrast free technique to image the lungs that is also used while the patient can breathe freely. It is based on the separation of the ventilation and perfusion signals, according to their frequency. Built on top of this is the Phase-Resolved Functional Lung MRI (PREFUL) which allows for the reconstruction of the breathing and cardiac cycle based on the phases of the acquired signal. The present study analysed different methods to extract the phase, to obtain the ventilation and perfusion maps and to threshold and detect the defects. It was found that the methods based on sine fitting and Morlet wavelet are the most promising, with the latter having the advantages of a variable window size and frequency. The most promising threshold for perfusion is the 75^{th} percentile * 0.6 and for ventilation the 90^{th} percentile * 0.4. Despite not correlating very well with the established methods, PREFUL analysis could still be useful in comparing different patients and tracking the progress of lung diseases.

Table of Contents

Acknowledgements **vii**

1 Introduction **1**
1-1 Context 1
1-2 Related work 3
1-3 Objective 4

2 Methods **5**
2-1 Data 5
2-2 Pre-processing 5
2-3 Analysis 6

3 Results **15**

4 Discussion and conclusions **23**

Bibliography **25**

List of Figures

2-1 Images before and after the bias field correction 6
2-2 Different masks 7
2-3 Images before and after the guided filter 7
2-4 Mean intensities per frame 8
2-5 Spectra 9
2-6 Ventilation and perfusion maps from FD 9
2-7 Fitted sine waves for phase extraction 10
2-8 STFT spectograms 11
2-9 Morlet wavelet 12
2-10 Morlet wavelet spectograms 12

3-1 Lungs and ROI signals reconstructed cycles comparison 16
3-2 Fractional and regional ventilation maps 16
3-3 Perfusion maps 17
3-4 Reconstructed cycles and corresponding maps for perfusion 17
3-5 Reconstructed cycles and corresponding maps for ventilation 18
3-6 Difference in the defect percentage 18
3-7 Difference between FD and PREFUL maps 19
3-8 Perfusion thresholding results 20
3-9 Ventilation thresholding results 21
3-10 Perfusion/ventilation maps compared to the reference scans 22

Acknowledgements

The present thesis concludes my two years of studying to obtain my Master's degree at TU Delft. I would not have been able to undertake this degree without the support of the committee that awarded me the TU Delft Excellence scholarship that helped me fund my studies and I would like to thank them from the bottom of my heart. This thesis is the product of the collaboration between me and my supervisors: Dr. Pierluigi Ciet, Dr. Frans Vos and Prof. dr. Harm Tiddens, to whom I would like to express my gratitude for supporting and encouraging me throughout the whole period in which I worked on this project. Special thanks go to my friends who made this stage of my life more enjoyable and who taught me how take everything more lightly . Last, but not least, I would like to thank my family for always believing that I can achieve whatever I set my mind to and for supporting me unconditionally.

Chapter 1

Introduction

1-1 Context

The primary function of the lungs is to perform the gas exchange in the alveoli, such that oxygen is delivered and carbon dioxide is eliminated in the blood [1]. This exchange is possible because of the lung ventilation, which is the action of replacing the gases in the lungs with fresh air from the atmosphere [2]. Another factor that influences the gas exchange is the lung perfusion, which describes the amount of blood that reaches the alveoli and how homogeneously is distributed in the lung. These two factors, ventilation and perfusion of the lungs are important physiological processes, that are affected by several pulmonary diseases [3]. Pulmonary diseases determine a mismatch in the ventilation/perfusion ratio due to the hypoxic vasoconstriction reflex. This physiological process occurs when areas of the lung parenchyma are not well ventilated and therefore causing hypoxia. To keep the gas exchange efficient in the alveoli, those areas are consequently less perfused. Therefore chronic hypoxia also determines hypo-perfusion. This effect is seen in several chronic lung diseases, such as asthma, cystic fibrosis (CF), pulmonary hypertension or chronic obstructive pulmonary disease (COPD) [4]. One of the most common chronic pulmonary disease is CF, an inherited genetic disease which affects the pancreas, liver and intestine, besides the lungs. It causes mucus plugging, infection and inflammation by changing the volume, viscosity and composition of the airways surface liquid [5]. COPD is described both by a change in the airway structure (bronchioectasis) and by destruction of parenchyma (emphysema) [6]. In both of these diseases, as well as in other chronic ones, following their progress is of great importance to effectively time the therapeutic interventions. In case of COPD, pulmonary blood flow impairment has been observed even in mild cases, so a perfusion assessment can lead to earlier detection and monitoring of the affliction [7].
There are several methods to diagnose and monitor chronic lung diseases. Spirometry is used to test the pulmonary function by measuring the volume or flow of air during inspiration and expiration. While it provides valuable insight into the disease evolution, it is still a global measurement which cannot give the level of detail and regional information requiered for a proper disease assessment. One of the most widespread modality for functional lung imaging

used to be SPECT/CT. However, it has several disadvantages, namely poor spatial resolution, usage of radioactive materials, which makes repetitive scans an issue, especially in children and pregnant women and patient discomfort. All these made CT a more attractive option for lung ventilation and perfusion assessment. Even though, CT is faster than SPECT and has a higher spatial resolution, it still poses the danger of radiation and it should be used with caution, especially in the case of periodic scans and in the case of children, who are more sensitive to radiation exposure than adults [8].

To overcome this problem, magnetic resonance imaging is used as a non-ionizing alternative to assess the regional lung ventilation and perfusion and there are three main functional imaging techniques employed for this goal. Dynamic contrast-enhanced MRI (DCE-MRI) is used to obtain perfusion maps by intravenously injecting contrast agents based on gadolinium, which provide contrast by shortening the T1 relaxation time. Besides the patient discomfort of breath hold and contrast injection, another disadvantage of DCE-MRI is that it sometimes can cause allergic reactions due to the administration of gadolinium. It is especially dangerous for patients with renal dysfunction since it can lead to a condition known as nephrogenic systemic fibrosis [9]. This is why DCE-MRI in children up to 1 year old should be avoided, since their kidneys are not yet fully developed [3]. An alternative to evaluate the lung perfusion is to use arterial spin labeling (ASL) MRI where the arterial blood water is magnetically tagged before entering the region of interest by applying a radiofrequency pulse which inverts the water protons. While ASL is a non-invasive technique which poses no risks for people allergic to contrast media, it has low signal-to-noise ratio and low temporal resolution which does not allow for scanning the whole lung volume in a reasonable time [9]. Regarding ventilation maps, they can be obtained by imaging the lungs after the patient inhaled hyperpolarized noble gas, such as ^{3}He or ^{129}Xe. This is a fast method that allows to monitor the ventilation changes in the lungs, but the production cost of the gases is high, it requires specialized hardware adapted for a different Larmor frequency and these tracers are not widely available [4]. For these reasons, this method is not commonly used in many health centers.

The disadvantages of these methods prompted the development of a new, non-contrast enhanced functional MRI technique to evaluate the regional ventilation and perfusion in the lungs, called Fourier decomposition MRI (FD-MRI) [9]. It brings together the advantages of having no need for breath-hold and no need for a contrast medium as well as being radiation-free. It is well known that the MR signal changes with the proton density and in lungs this fluctuates according to the respiration motion because air goes in and out. It has been shown that the changes in the MR signal correlate with changes in the lung volume [10], but since there is a fixed volume of tissue, the only variable is the volume of air entering or leaving the lungs. When air is entering the lungs, their density decreases, as tissue is being replaced by air. This decrease in density will lead to a decrease in signal, which can then be used to calculate the change in air volume, which is the ventilation [11]. The opposite is true for the expiration, when the air is expelled the lung density and MR signal increase. Another factor that contributes to the signal change is the cardiac cycle. Thus, by acquiring a time series of a coronal slice, the MR signal change that is observed in time is given both by the respiration motion and the cardiac cycle.

Because the frequency of the respiratory movement of 16 breaths per minute on average is different than the heart rate of 60-80 beats per minute for adults, the signals contributing to these cycles can be separated in the frequency domain. For this, the time series has to be acquired with a rate at least double of the highest frequency in the spectrum. By applying a Fourier transform, the peaks for the respiration and cardiac movement can be identified in the

spectrum and the signals can be separated to obtain ventilation and perfusion information. The final ventilation and perfusion maps are obtained by integrating the time series over the two separate peaks and the possible defects identified.

1-2 Related work

Fourier-decomposition MRI has first been described by Bauman *et al.* [9] as a non-contrast-enhanced MRI technique to obtain lung ventilation and perfusion maps. Because of its many advantages, like the lack of radiation, the fact that it is non invasive and it does not require breath hold, FD-MRI became a promising technique to assess lung diseases, especially for pediatric patients. Before it could be implemented in the clinical routine, further testing and validation were necessary. First such tests were performed on pigs and FD-MRI was first compared with SPECT-CT [12] and then with hyperpolarized ^{3}He and DCE-MRI [3]. They found that the agreement between the different methods compared was visually good and the defective regions from the FD maps had significantly different values than the healthy regions and thus they could be identified.
Any new diagnostic method needs to be validated against well established techniques and for different scenarios. FD-MRI has been compared with DCE-MRI in CF [5] and lung cancer [13] patients, with ^{3}He MRI in COPD [6] and asthma [14] and with ^{19}F MRI in COPD [15]. Its feasibility was also tested in the detection of chronic allograft dysfunction [16] and kidney perfusion [17]. Besides this, there have been efforts done to quantify the maps [18, 19], for easier comparison. The results showed that the FD-MRI images have lower quality than DCE-MRI. The correlation was good with all the major defects being identified by FD-MRI but the small ones generated false positives and negatives. The correlation was not the best between FD-MRI and hyperpolarized gasses imaging either because of the different information the two methods capture and provide. Overall, the FD-MRI showed its potential of being used to identify different lung afflictions and even renal diseases.
Starting from the acquisition of free-breathing time series and from the FD algorithm, Voskrebenzev *et al.* [20] introduced a new post processing method to fully reconstruct the cardiac and ventilation cycles and analyze the data dynamically. The method is based on sorting the frames from the time series based on their estimated phase to resolve the cycle with a higher temporal resolution and it is named Phase-Resolved Functional Lung (PREFUL) MRI. This means that from approximately 65s of acquired images spanning over multiple breathing or cardiac cycles only one cycle is reconstructed with all the images sorted according to the phase they belong to. This enabled the calculation of new quantities, like time-to-peak, regional ventilation, pulmonary transit wave time, as well as ventilation and perfusion defect maps.
Like the original FD method, the PREFUL one has been tested against other established techniques to assess the ventilation and perfusion of the lungs in several diseases. It has been tested against DCE-MRI [7, 21], hyperpolarized ^{129}Xe [22, 23] and in COPD [24], chronic lung allograft dysfunction [25] and chronic thromboembolic hypertension treatment [26]. The results are similar to the ones that have been found when testing FD-MRI. PREFUL MRI is promising in being a reliable diagnosis tool for a wide range of lung afflictions, especially when calculating the new dynamic quantities. The correlation with the other diagnosis tools is not excellent, but this is mostly due to the differences in their working principles. This shows that the results from all these techniques should be interpreted and used in a complementary way and analysed independently too.

1-3 Objective

The goal of this study is to take a look at how the PREFUL and FD analysis are being done and described in literature and from all the options available to obtain the ventilation or perfusion maps and to segment the defects, propose a processing pipeline that is generally applicable. Besides this, the study aims to find out if there is another, maybe more intuitive way to perform the phase extraction step in the PREFUL algorithm than the one described in the original paper on this topic.

Chapter 2

Methods

2-1 Data

The data were acquired from Erasmus Medical Center in Rotterdam and the regional medical center in Treviso, Italy. In total 7 subjects from Erasmus and 2 subjects from Treviso were analysed. The last 2 have been scanned twice at two different dates and the second acquisition is accompanied by expiratory CT scans obtained in the same day. The scans from Erasmus MC were acquired from a GE MEDICAL SYSTEMS machine with an SPGR sequence. The FD data has the following characteristics: TR=2.3ms, TE=0.8ms, slice thickness=15mm, pixel spacing=1.95x1.95mm, matrix size=128x128. The expiratory MRI scan has the following characteristics: TR=1.3ms, TE=0.6ms, slice thickness=3mm, pixel spacing=1.4x1.4mm, matrix size=120x120. The data from Treviso was acquired from a SIEMENS scanner with a FLASH sequence. Other characteristics for the FD data are: TR=90.7ms, TE=1ms, slice thickness= 15mm, pixel spacing=1.95x1.95mm, matrix size= 128x129. The reference expiratory MRI from Treviso was acquired with a Spiral VIBE sequence and has: TR=3.3ms, TE=0.1ms, slice thickness=2.5mm, pixel spacing=2.08x2.08mm and matrix size=288x288. The contrast MRI scans were acquired with the 3D TWIST sequence and are characterised by: TR=1.7ms, TE=0.6ms, slice thickness=3.09mm, pixel spacing=3.12x3.12mm, matrix size=160x50.

2-2 Pre-processing

Before the images were analysed some pre-processing was required to ensure they are all standardised. The first step was to convert them from the DICOM format to NIfTI. They were sorted according to the acquisition time stored in the DICOM metadata and named accordingly. The next step was to correct for the inhomogeneities present in the intensities of the MRI image. This non-uniformity is caused by the inhomogeneities in the magnetic field which lead to the corruption of the images such that the grey levels for the same tissue vary in space [27]. To solve this issue, the N4 bias field correction algorithm from SimpleITK

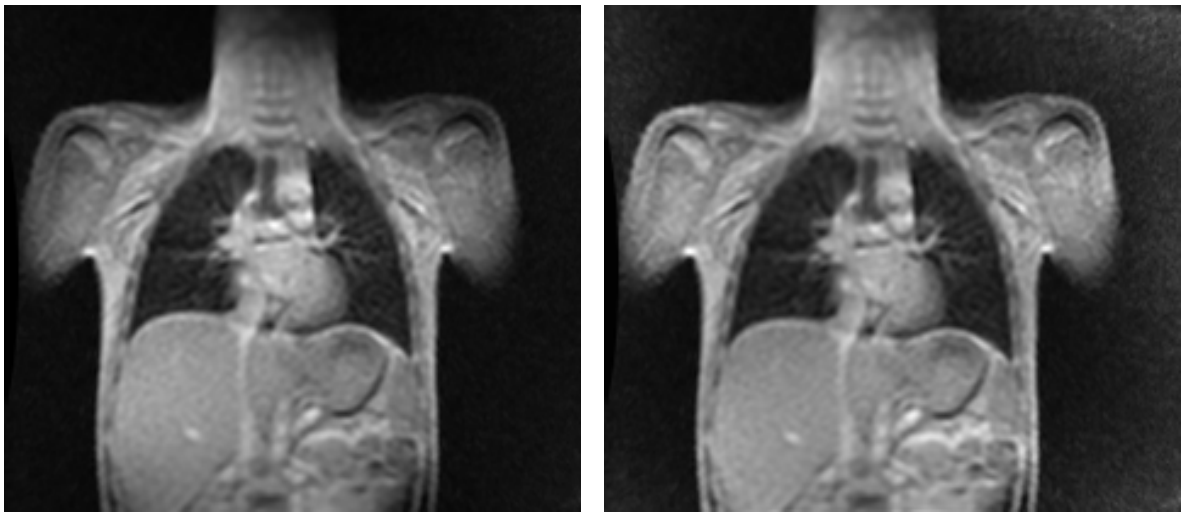

(a) Before the N4bias correction **(b)** After the N4bias correction

Figure 2-1: Images before and after the bias field correction

[28, 29, 30] was applied and the effect can be seen in 2-1. This was done in the Biomedical Imaging Group Rotterdam (BIGR) CPU cluster along with the registration. The elastix software [31, 32] was used for the non-rigid registration of all the frames to a frame in mid-respiration. This was done for each slice. Once all these were done, the two lungs, the chest, the region around the diaphragm and aorta, where present, were manually segmented separately in 3DSlicer [33]. The diaphragm region of interest (ROI) and the aorta were segmented because the mean signal from these regions was used in a later step of the algorithm where the phase is extracted. Some examples are in 2-2. The last step in the pre-processing was smoothing the images with a guided filter, which is an edge-preserving filtering technique that outputs similar results to the bilateral filter, but is faster [34].

2-3 Analysis

After pre-processing, the first 20 images were removed from the analysis because they were acquired while the steady state had not been reached. The steady state occurs when the radio frequency pulses are delivered faster than the time it takes for the longitudinal magnetization to recover. The amount it regains is equal to the amount of transversal magnetization induced by the next pulse and the spins become static and saturated [35]. By spatially averaging each frame, a signal that captures the variation of the series in time was obtained. This signal was high-pass filtered with a cut-off frequency of 0.7 Hz to get the perfusion signal and the same threshold was used for low-pass filtering it to get the ventilation signal. An example of the signals obtained by spatially averaging the smoothed images, the low-pass and high-pass filtered ones can be seen in 2-4. The frequency of each signal was determined after it had been Fourier transformed and the peak with the highest amplitude has been identified. The spectra and the highest peak for each of them can be seen in 2-5. The final step for the FD analysis was to integrate the spectra from each voxel over the full width half maximum of the previously identified peak to obtain the perfusion or ventilation map, depicted in 2-6.

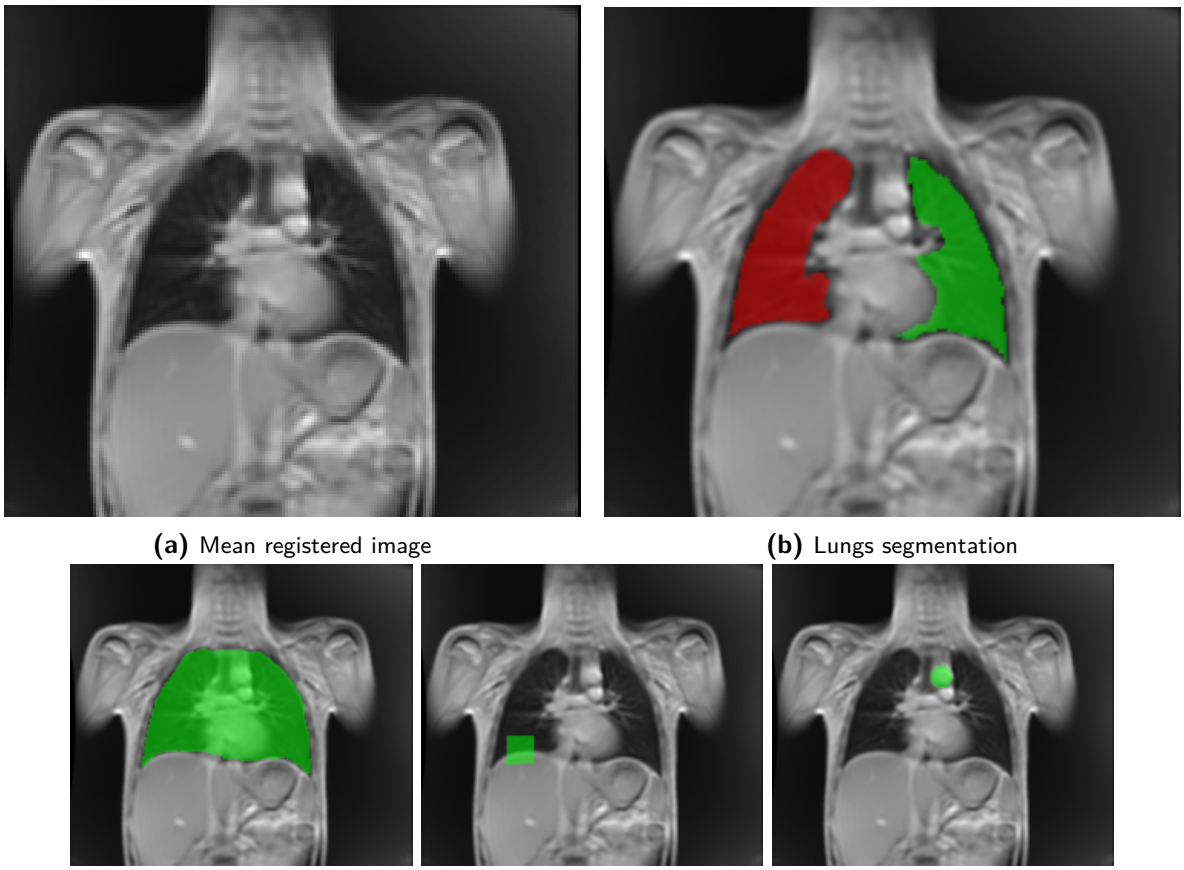

(a) Mean registered image

(b) Lungs segmentation

(c) Chest segmentation

(d) Diaphragm region segmentation

(e) Aorta segmentation

Figure 2-2: Different masks

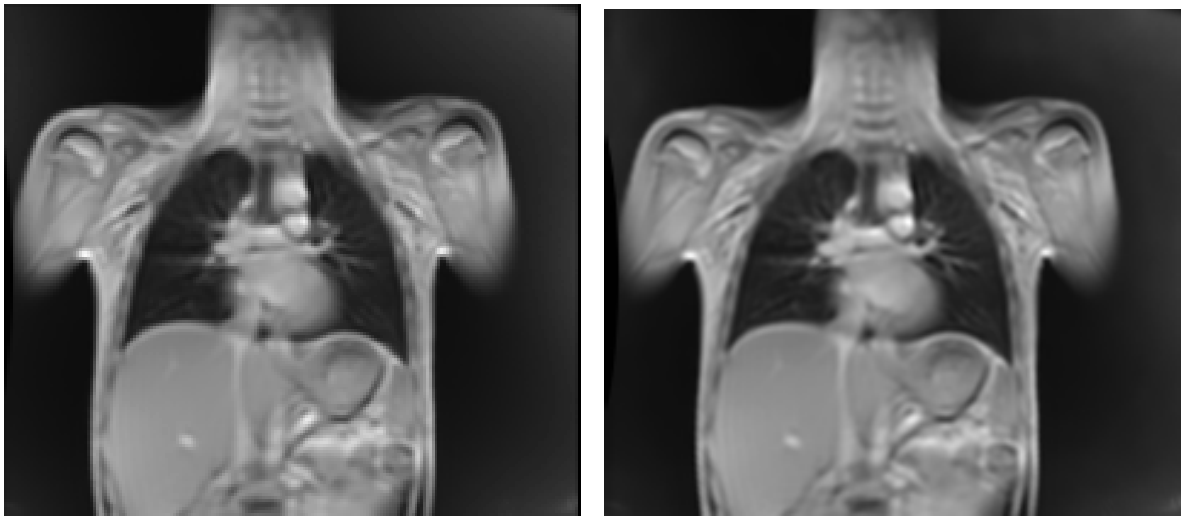

(a) Mean image before filtering

(b) Guided filtered image

Figure 2-3: Images before and after the guided filter

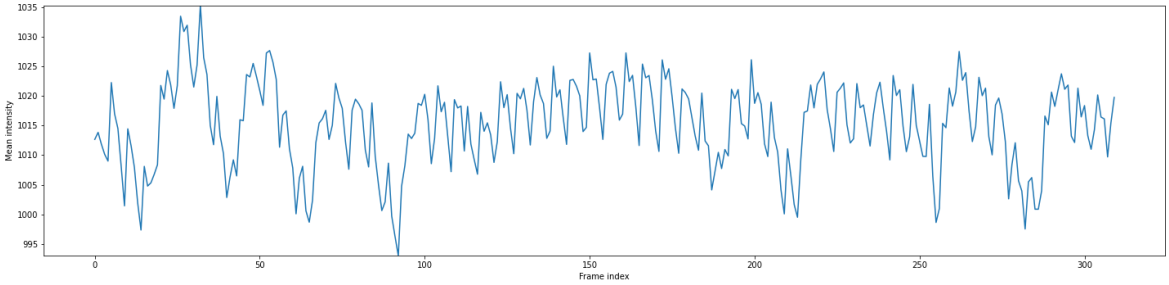

(a) Mean intensity per frame

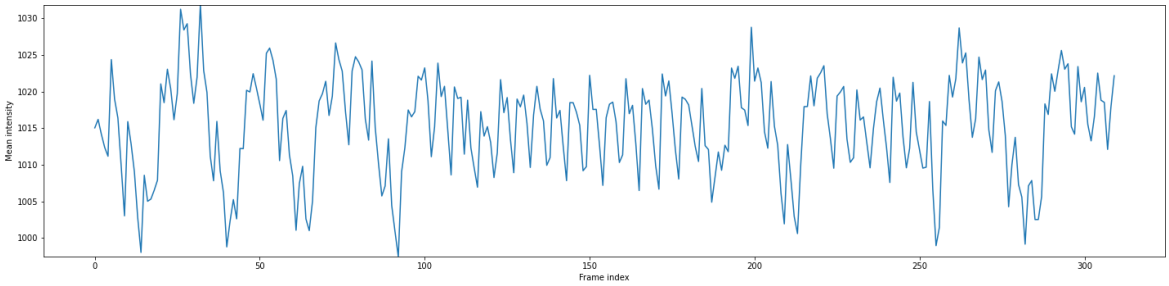

(b) Mean intensity per frame after removing very low frequencies

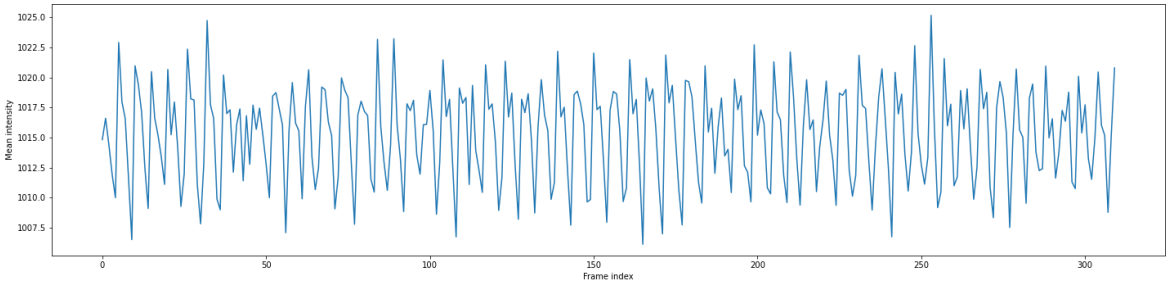

(c) Mean intensity per frame after the high-pass filter

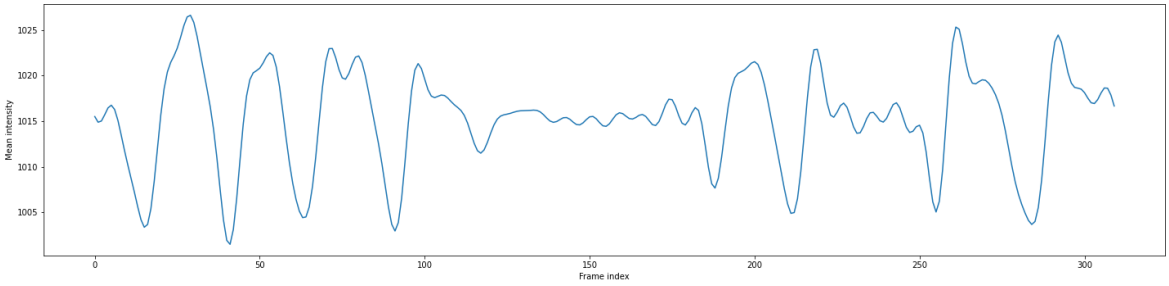

(d) Mean intensity per frame after the low-pass filter

Figure 2-4: Mean intensities per frame

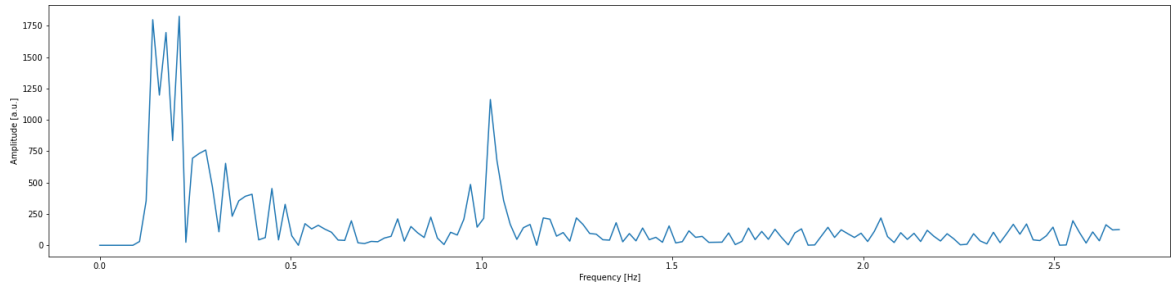

(a) Spectrum of the initial signal

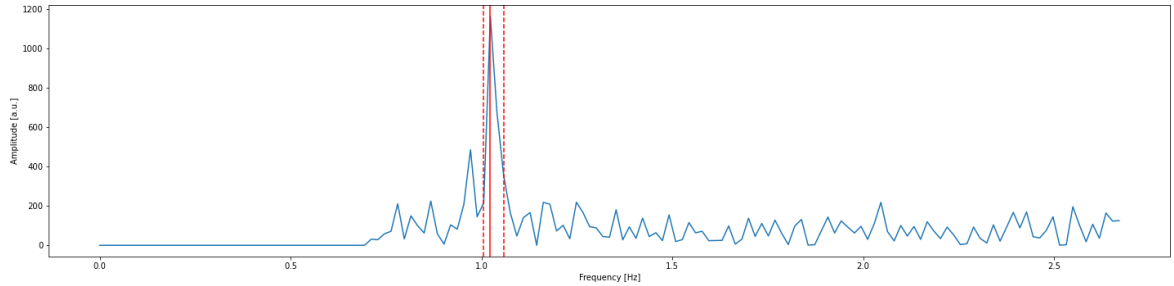

(b) Perfusion spectrum

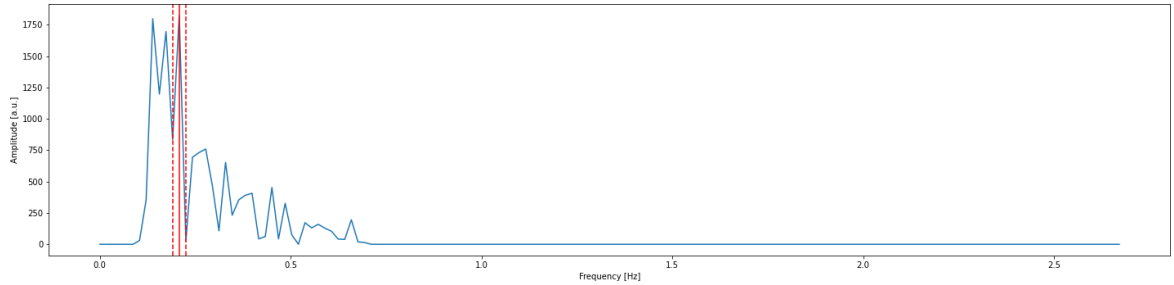

(c) Ventilation spectrum

Figure 2-5: Spectra

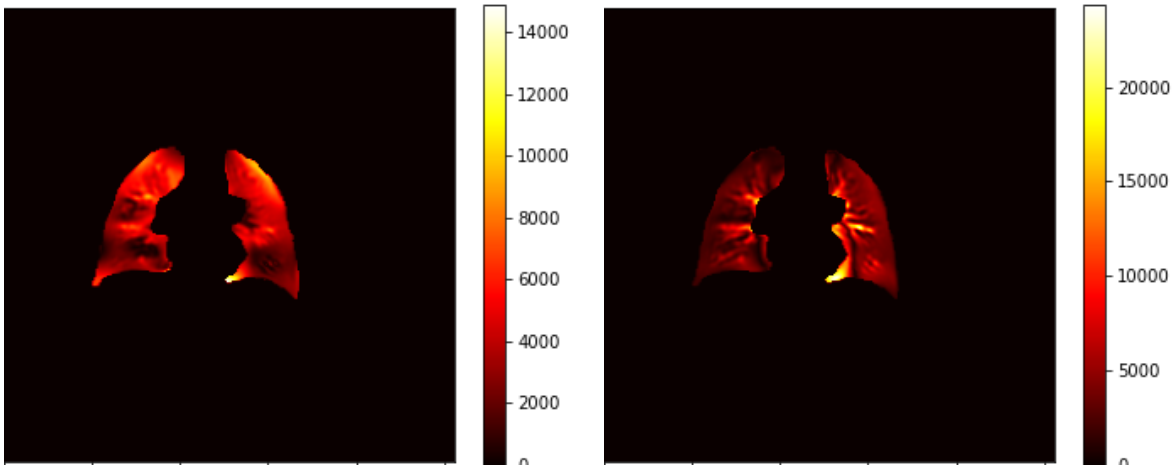

(a) Ventilation map **(b)** Perfusion map

Figure 2-6: Ventilation and perfusion maps from FD

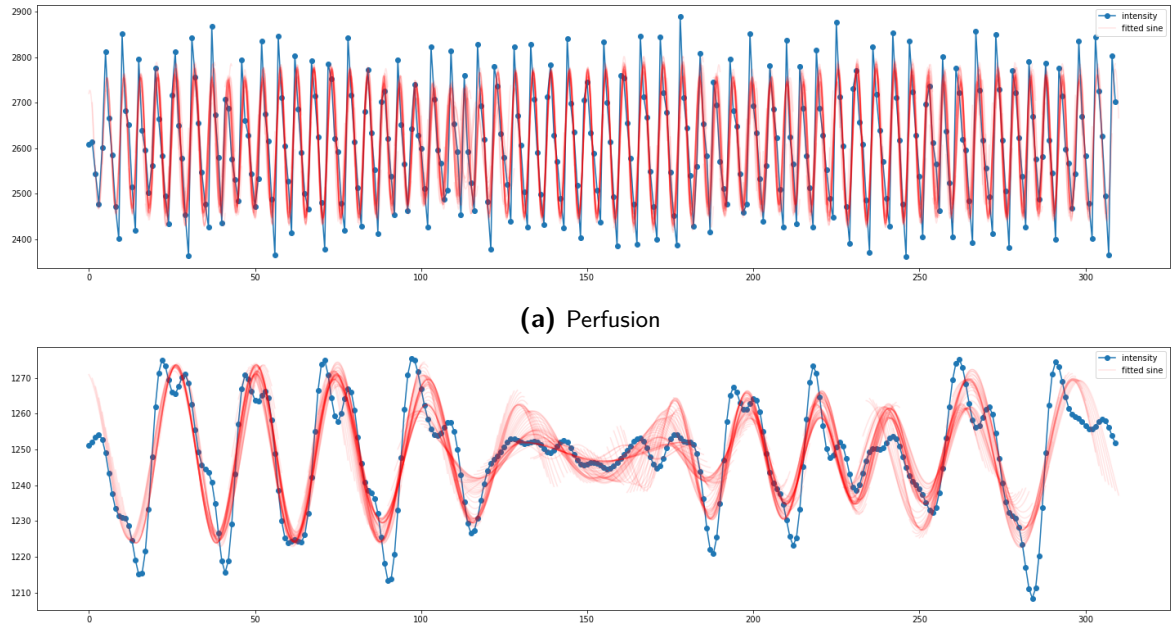

(a) Perfusion

(b) Ventilation

Figure 2-7: Fitted sine waves for phase extraction

The starting point for the PREFUL method was having the signal separated into ventilation and perfusion signals, as described before. The ventilation signal was obtained from the diaphragm ROI, according to literature, but the signal coming from the lungs was also analysed to observe the differences. For perfusion, the signal was obtained from the aorta in the frames where it was present or from the lungs, otherwise. In this case the signal from the lungs was analysed as well for comparison. On each of these signals, three methods to extract the phase of each time point were studied.

The first method to extract the phase is the one described in the original paper about PREFUL [20] and it involves a sine wave to be fitted on windows of the signal. These windows are defined as the signal between two peaks in the paper by Voskrebenzev *et al.*, but because they proved to have too few time points for the fitting algorithm to work, the length of a window was set to 20 points for perfusion and to 50 points for ventilation. The stride of sliding the window is one time point. Every time a point was inside the sliding window its phase was determined from the fit sine wave. The final phase for each point was estimated as the normalized phase over all the times the point was covered by the window. The sine waves fitted on the two signals can be seen in 2-7. The method described here is the one used for perfusion in the original PREFUL paper. There, for ventilation, a model function was used to separate the signal into inspiration and expiration and from there calculate the phase. In this thesis, the same algorithm described above for perfusion was used for the ventilation signal as well .

The next two methods of extracting the phases were based on time-frequency analysis, namely short-time Fourier transform (stft) and Morlet wavelet transform. This type of analysis is often used to manipulate non-stationary signals which are not characterized by one value of the frequency, but for which it varies in time, as it is the case in this study. Fourier analysis describes the frequency components of the signal globally and assumes it is infinite or periodic.

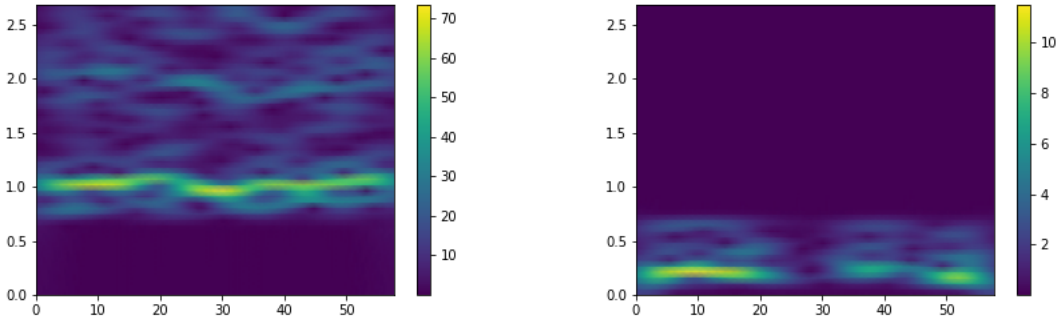

(a) Perfusion **(b)** Ventilation

Figure 2-8: STFT spectograms

The time-frequency analysis takes into consideration the signal variability and assumes that there are short windows within it where the frequency is constant. Therefore, the signal can be simultaneously analysed both in time and frequency and increasing the resolution in one domain will decrease it in the other. The first method was the short-time Fourier transform, where the signal is divided in small windows and for each of them the Fourier transform is computed. Particularly, the Gabor transform was used, which means that the window has the shape of a Gaussian function which is slid over the signal. At each time point, the window is multiplied with the signal covered by it. This ensures that the points closest to the point being analysed have the highest weight. The complex coefficients are used to obtain the amplitude and the phase for each point. Once the run-through was complete, a spectrogram was created by plotting the amplitude intensity on a graph where time is on the x-axis and the frequency is on the y-axis, as seen in fig 2-8. As the colours indicate, in this example, the highest amplitude for perfusion corresponds to a frequency of around 1 Hz and for ventilation it is around 0.23 Hz. The standard deviation of the Gaussian window was set to 20 and the number of points it covers from the signal to 100. The second way that the signal was analysed in the time and frequency domains was by using a Morlet wavelet, which can be seen in 2-9. The signal was convolved with the wavelet whose frequency and width are varied by taking the values from a user-defined interval. This is also the main difference between the two time-frequency analysis methods. In case of the stft the width of the window is fixed and is given by the standard deviation of the Gaussian. For the Morlet wavelet, the width varies according to the frequency of the wavelet currently used: the higher the frequency, the narrower the window and vice-versa. The width of the Morlet wavelet for a certain frequency is given by:

$$s = w * fs/(2 * f * \pi) \tag{2-1}$$

where w is the central frequency, fs is the sampling frequency and f is the frequency for which the width is being calculated and it can take values between zero and half of the sampling frequency, according to the Nyquist theorem. From the complex coefficients that result from the convolution, the amplitude and the phase were calculated and a spectrogram was created, similarly to the short-time Fourier transform, as seen in 2-10. For both methods, for each time point, the frequency with the highest amplitude was picked and its corresponding phase was assigned to that particular point.

Figure 2-9: Morlet wavelet

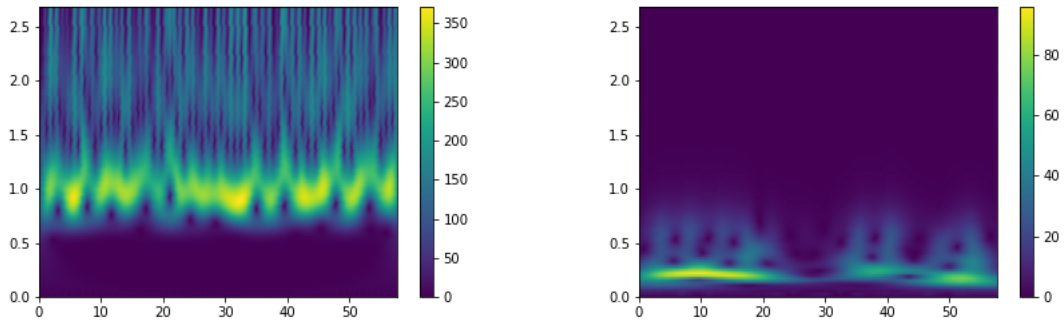

(a) Perfusion **(b)** Ventilation

Figure 2-10: Morlet wavelet spectograms

For each of the signals, first the phase was extracted for each time point with all three methods, one at a time. Then the values were sorted and interpolated on a regular grid of 60 points. The order of the sorted phases was used to sort and then interpolate the frames too into one cycle. From this, several characteristics can be extracted, like time-to-peak (TTP), pulmonary perfusion time or flow volume loops, but also the defect maps. For perfusion, the defect maps were calculated in two ways. The first one was by taking the difference between the frames corresponding to the maximum value and the minimum value in the cycle obtained by ordering the phases [36]. The second approach was to find the index of the phase with the maximum signal intensity for each voxel in the lung parenchyma and then to choose the frame corresponding to the phase with the most occurrences [21]. For ventilation, the maps were calculated as fractional ventilation (FV) and regional ventilation (RV), which are described in 2-2 and 2-3, respectively:

$$FV = \frac{S_{exp} - S_{insp}}{S_{exp}} \tag{2-2}$$

$$RV = \frac{S_{mid}}{S_{insp}} - \frac{S_{mid}}{S_{exp}} \tag{2-3}$$

The expiratory image (S_{exp}) is the frame corresponding to the phase with the highest intensity and the inspiratory image (S_{insp}) corresponds to the lowest intensity in the reconstructed cycle. The signal in the middle (S_{mid}) comes from the middle point between the expiratory and inspiratory images.
The defects of perfusion and ventilation were assessed by applying a threshold to their respective, previously acquired maps. The were several thresholds taken from literature and their results compared with each other to find one that is generally applicable.
For the perfusion-weighted values the thresholds used were: the median value - 0.5 * standard deviation [20], the 75^{th} percentile * 0.6 [7, 36, 21, 26], the median value - 0.75 * standard deviation [37].
Similarly to the perfusion defect percentage, the ventilation defect percentage was determined in literature using several thresholds, such as: median value - 4 * standard deviation [20], the 75^{th} percentile of all the RV values * 0.7 [36], the median value - 1.75 * standard deviation [37] or the 90th percentile of all the RV values * 0.4 [38, 22, 39]. In one study [23] the ventilation defect percentage was determined after the k-means algorithm was applied to the fractional ventilation map and the first 5 clusters in terms of intensity were deemed defective. In this study, the k-means algorithm was applied with 5 clusters and the second one was chosen as the defective one after they were sorted in ascending order of their centre value. In this case the k-means algorithm was applied to both ventilation and perfusion maps.

Chapter 3

Results

In this chapter the results of the experiments performed are presented. Their aim was to compare several of the characteristics of the PREFUL algorithm and to determine which ones were the most appropriate to be used in the Erasmus MC pipeline. For this goal, the results obtained from the lungs signal were compared to the results obtained from the ROIs signal. Other comparisons were done between the three methods for phase extraction, the different thresholds to determine the defect percentage and between PREFUL and FD results.
First of all, the signal used to extract the phases for the PREFUL algorithm was obtained from the diaphragm ROI for ventilation and from the aorta for perfusion. In many slices the aorta was not visible and then the signal from the lungs was used instead. When the results from the aorta and diaphragm ROI were compared with the results from the lungs, little differences were visible in the reconstructed cycle for the sine fitting method and the Morlet wavelet one. This can be seen in 3-1 and it shows that the signal from the lungs can be used in the analysis, therefore saving time by removing the need for extra segmentations. The aorta would still need to be segmented for further characterization, like quantification or TTP.
When it comes to ways of visualising the ventilation maps, between the fractional and regional ventilation, in most cases the latter provided a better contrast, wider intensity range and ease of observing the defects, as it can be seen in 3-2. For perfusion, the method that defined it as the difference between the frames corresponding to the maximum and the minimum values in the reconstructed cycle was chosen for further analysis. Despite the fact the both methods had similar outputs, as it can be seen in 3-3, the choice was made in collaboration with the radiologist that supervised this study who visually assessed both methods. Besides this, the chosen method is most commonly used in literature and in some cases it is visually more similar to the contrast-enhanced MRI scans.
The three methods of extracting the phases output similar looking perfusion and ventilation maps, despite the fact that the reconstructed cycles look different. An example of the difference between the cycles and the similarity of the maps can be seen in 3-4 and 3-5. The stft results were the most different visually compared to the other two methods, which was also emphasised in the differences between the mean defect percentages across all the thresholds. For perfusion, the overall difference between PREFUL and sftf was 2.10% and between

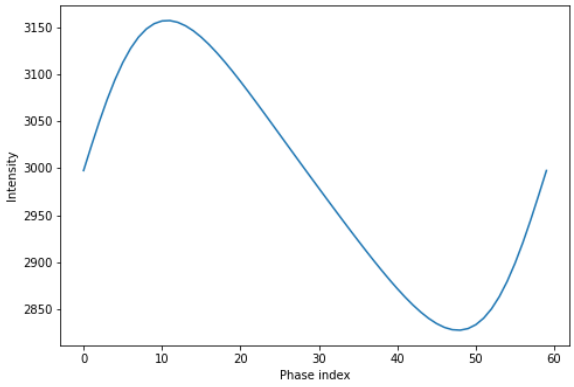

(a) Cycle reconstructed from the aorta ROI

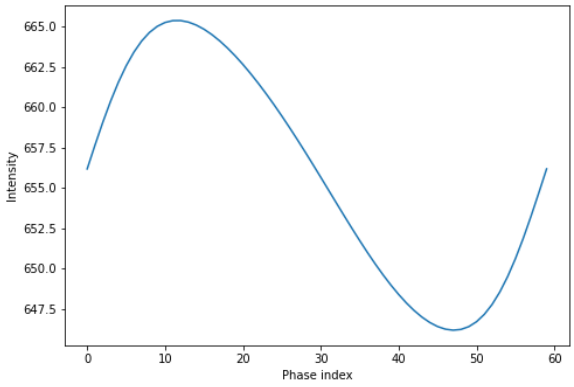

(b) Perfusion cycle reconstructed from the lungs

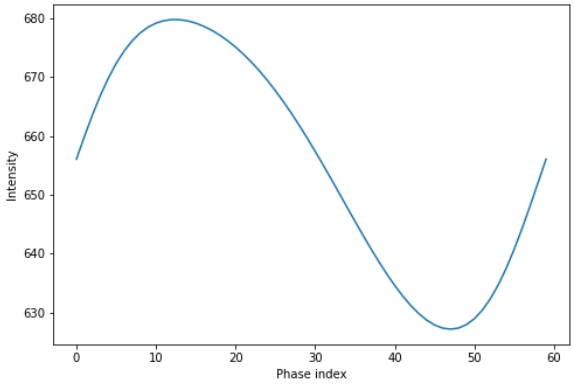

(c) Cycle reconstructed from the diaphragm ROI

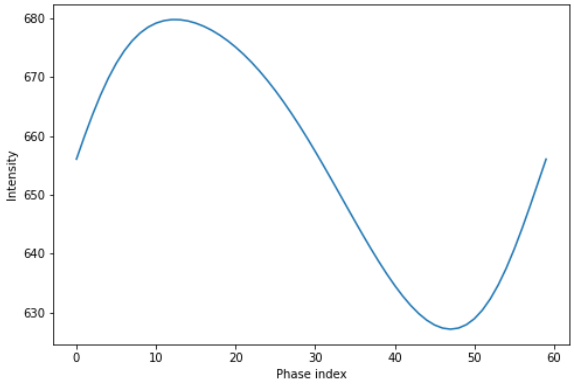

(d) Ventilation cycle reconstructed from the lungs

Figure 3-1: Lungs and ROI signals reconstructed cycles comparison

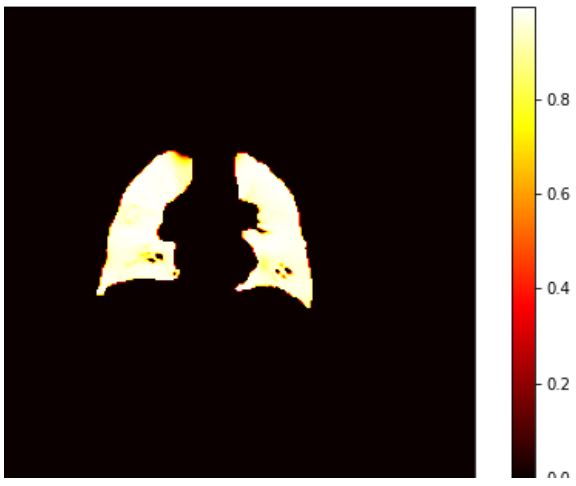

(a) Fractional ventilation map

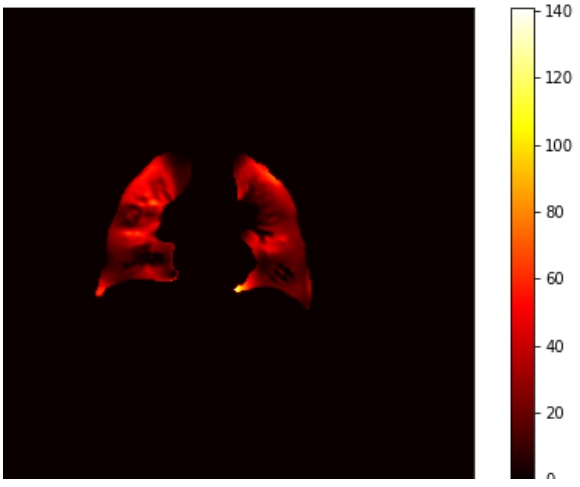

(b) Regional ventilation map

Figure 3-2: Fractional and regional ventilation maps

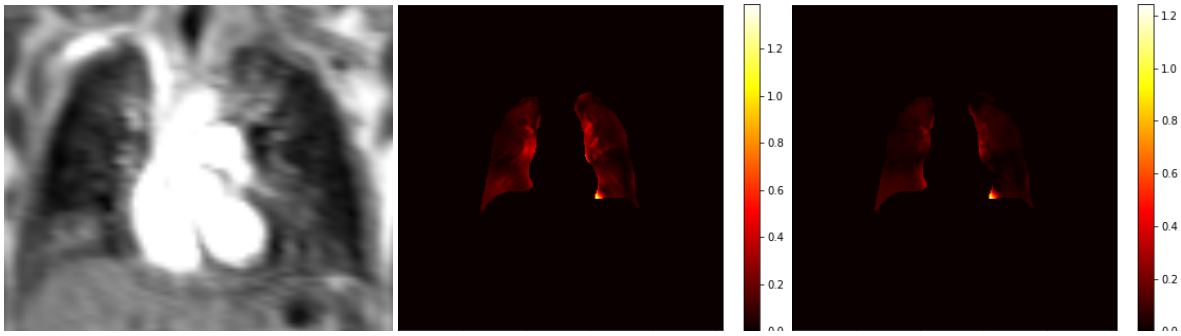

(a) Contrast-enhanced MRI **(b)** Perfusion map - method 1 **(c)** Perfusion map - method 2

Figure 3-3: Perfusion maps

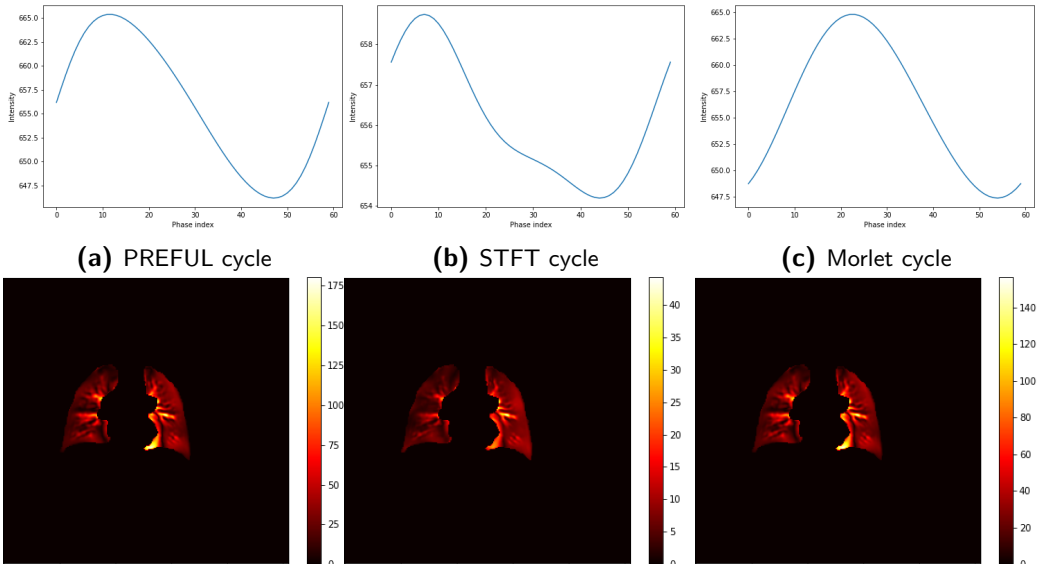

(a) PREFUL cycle **(b)** STFT cycle **(c)** Morlet cycle

(d) PREFUL perfusion map **(e)** STFT perfusion map **(f)** Morlet perfusion map

Figure 3-4: Reconstructed cycles and corresponding maps for perfusion

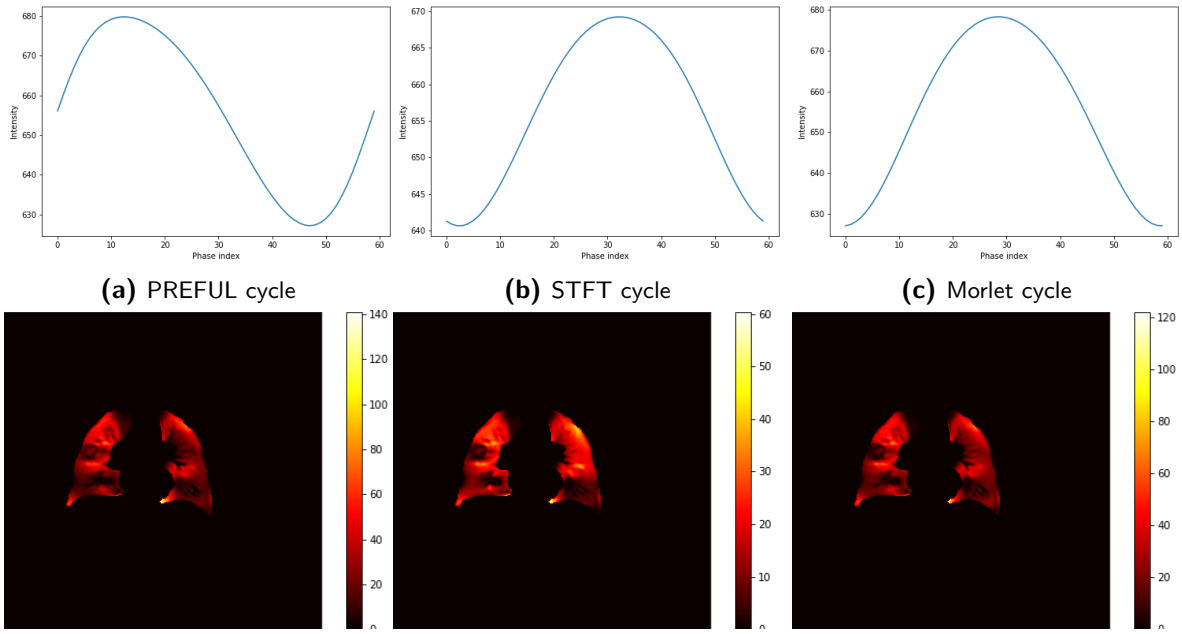

(a) PREFUL cycle **(b)** STFT cycle **(c)** Morlet cycle

(d) PREFUL map **(e)** STFT map **(f)** Morlet map

Figure 3-5: Reconstructed cycles and corresponding maps for ventilation

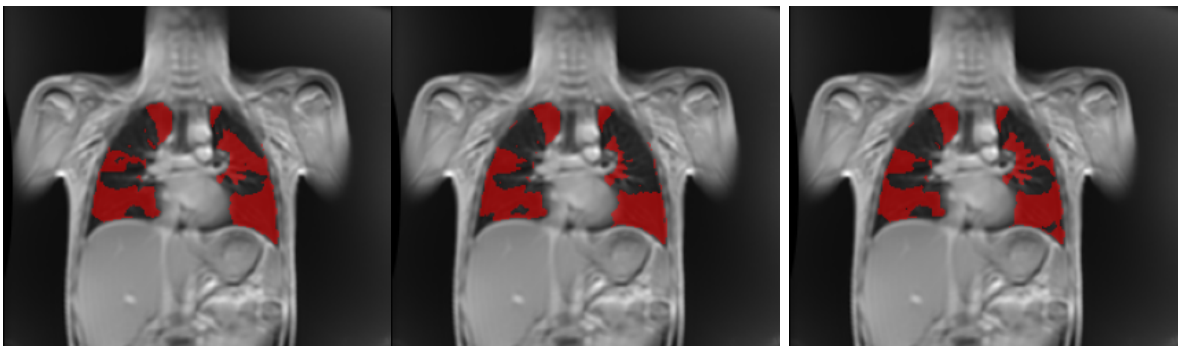

(a) PREFUL defect map **(b)** STFT defect map **(c)** Morlet defect map

Figure 3-6: Difference in the defect percentage

PREFUL and Morlet 1.22%, while for ventilation the PREFUL and stft showed a difference of 1.72% and between PREFUL and Morlet there was one of 0.77%. These differences are also illustrated in 3-6. Even though visually the output maps from FD were similar to the ones from PREFUL, as shown in 3-7 the defect percentages showed significant differences, especially in the ventilation case. These were 2.1% for perfusion and 5.68% for ventilation.
Differences in defect percentages were also present in the results output by applying different thresholds. In 3-8 it can be seen the results of applying the aforementioned thresholds on the same perfusion map obtained with the original PREFUL method and in 3-9 the same thing is illustrated for the regional ventilation maps resulted from the original PREFUL method as well.
The results obtained with this algorithm were compared with expiratory MRI reference and CT scans for ventilation and with contrast-enhanced MRI scans for perfusion. One example

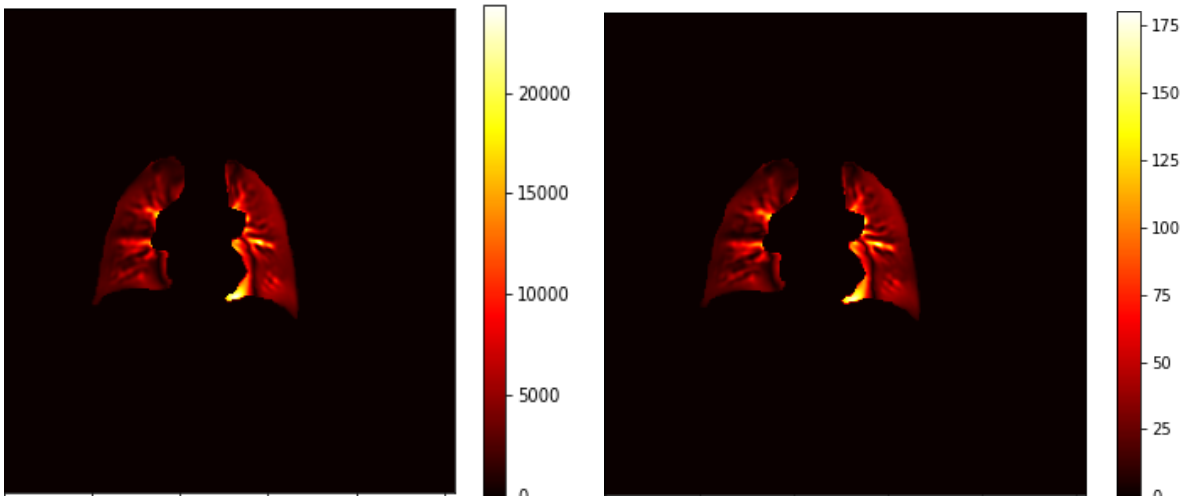

(a) FD perfusion map **(b)** PREFUL perfusion map

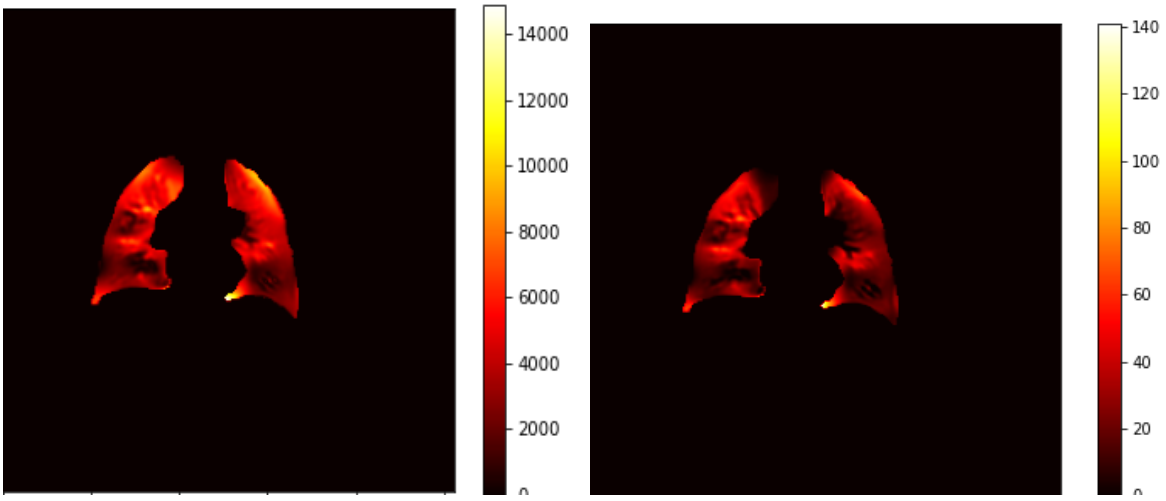

(c) FD ventilation map **(d)** PREFUL ventilation map

Figure 3-7: Difference between FD and PREFUL maps

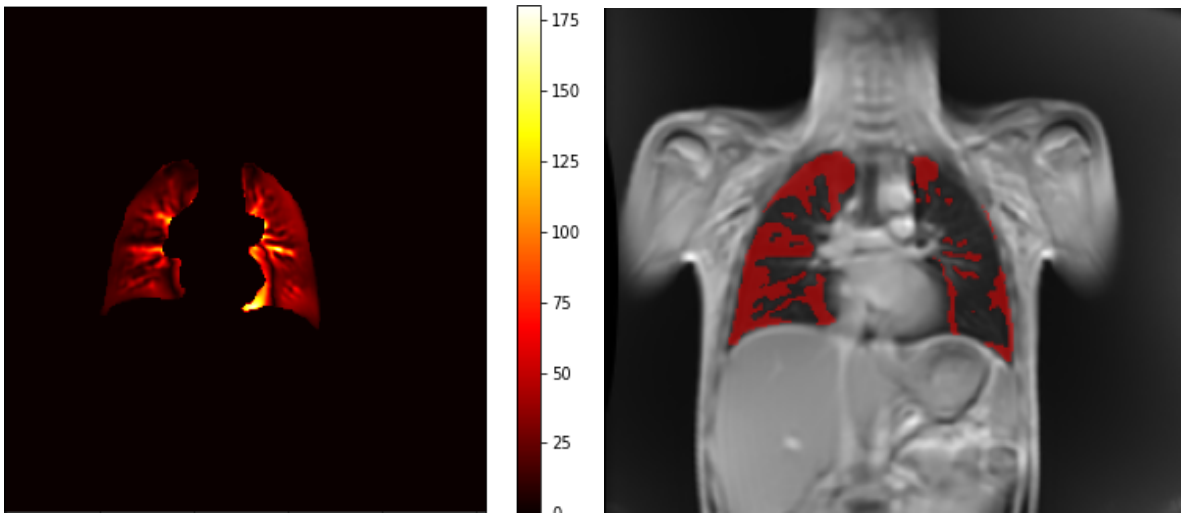

(a) PREFUL perfusion map

(b) 75th percentile * 0.6

(c) Median value - 0.5*std

(d) K-means

Figure 3-8: Perfusion thresholding results

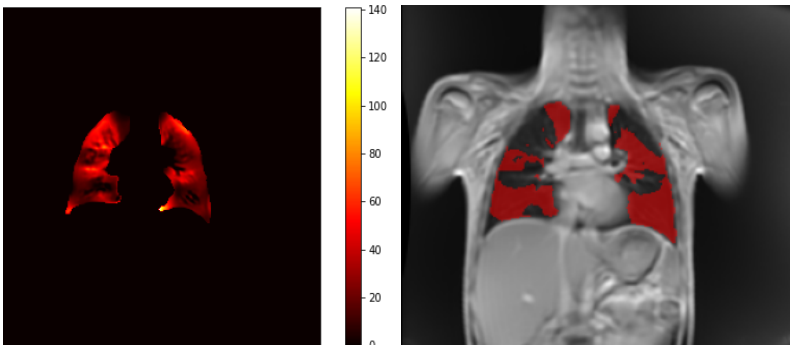

(a) PREFUL ventilation map **(b)** 75th percentile * 0.7

(c) Median value - 1.75*std **(d)** Median value - 4*std

(e) 90th percentile * 0.4 **(f)** K-means

Figure 3-9: Ventilation thresholding results

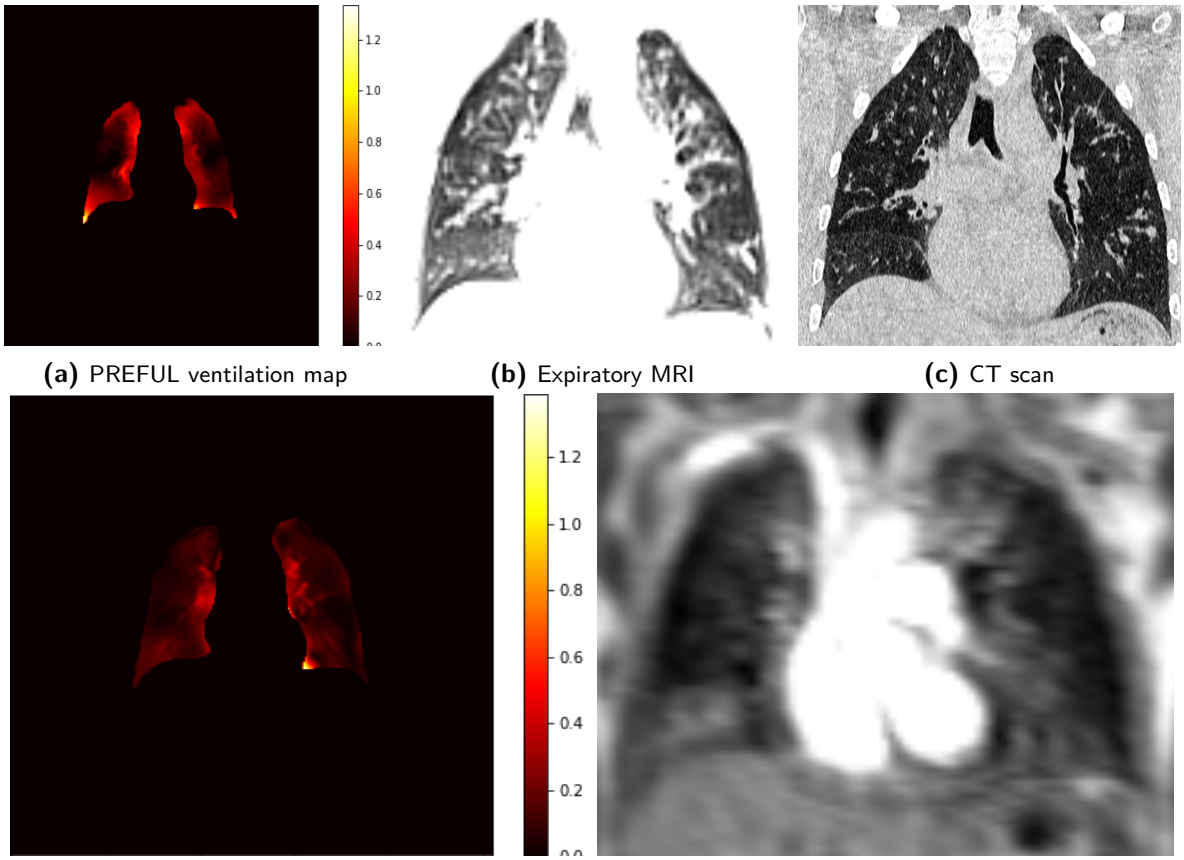

(a) PREFUL ventilation map **(b)** Expiratory MRI **(c)** CT scan

(d) PREFUL perfusion map **(e)** Contrast-enhanced MRI

Figure 3-10: Perfusion/ventilation maps compared to the reference scans

can be seen in 3-10. One of the CT scans was analysed with the Myrian 2.9.2 software [40] where the lungs as well as the low attenuation regions with HU between -856 and -950 had been segmented. The defect percentage obtained with this method was 26.38% and the mean one resulted from the PREFUL analysis on the same patient was 49.36%. Looking at the results of the three methods to extract the phase with the threshold of 90^{th} percentile * 0.4, the values of defect percentages are very close to each other: 49.86% for the sine fit method, 48.01% for stft and 50.22% for the wavelet transform, but still far from the 26.38% obtained from the CT scan.

Chapter 4

Discussion and conclusions

In this study, different aspects of the PREFUL algorithm that measures properties of lung perfusion and ventilation were analysed. I studied methods for extracting the phase, thresholds for the defect assessment, defect map definitions and comparison with the FD method. Taking a step away from the original description of the PREFUL algorithm, the same steps were used for the perfusion and the ventilation analysis with satisfactory results. Besides this, it has been found that using the signal from the lungs or the signal from an ROI, be it the aorta or the diaphragm region, outputs almost identical results for two of the phase extraction methods. Therefore, to simplify the whole process, only the lungs need to be segmented when there is no quantitative analysis being done which would require the segmentation of blood vessels.

Three methods of retrieving the phase of each point in the signal have been implemented: the original method described in the paper about PREFUL based on sine fitting and two methods based on time-frequency analysis: short-time Fourier transform and the Morlet wavelet transform. The ordering of intensities corresponding to the detected phases is different for each method, resulting in cycles with different shapes. The reconstructed cycle with the original algorithm looks very similar to a sine wave, which is not surprising given the fact it was obtained by fitting one to the signal. The cycle obtained with a Morlet wavelet often times resembles a bell-shaped plot, similar to the Gaussian envelope of the wavelet. The stft cycle shows the most variation, having different shapes for different data or even slices of the same scan. The stft results are also the furthest away from the other two methods in terms of the values of the defect percentages. The disadvantage of the sine fitting method is that the window length is fixed and the effect of varying has not been studied. The Morlet wavelet combines the advantages of a variable window size and frequency value, but these have yet to be quantified and the wavelet proven worthier than the other method.

When it comes to how the defect maps are defined, regional ventilation was chosen opposed to fractional ventilation. For perfusion, the map was defined as the difference between the frames corresponding to the maximum and the minimum point in the reconstructed cycle, as opposed to the frame corresponding to the most common phase. The thresholds to detect the defects were applied on these two types of maps. A the threshold of 75^{th} percentile * 0.6 appears to be the closest to what is visible in the perfusion map. For the ventilation

assessment, the 90^{th} percentile * 0.4 looks like the most promising threshold to segment ventilation defect maps. When the segmentation results are put against the reference scans, the former are consistently overestimating the defects, both from a visual point of view, as well as quantitatively, as showed by the comparison with the CT data. It is a complex issue to find the correct or true position and amount of defects given the fact that each modality is measuring different properties, i.e. MRI the magnetization and CT the X-ray absorption. Overall, the position of the low ventilated and perfused areas is similar throughout all the modalities, but the amount and exact location are varying. This is also a limitation of this study and of FD methods in general. The lack of a very good correlation between the output and the reference scans makes the defect assessment a complicated task.
Another limitation of this study that can be tackled in the future is the lack of lungs and defect segmentations for the reference scans. With these a quantitative comparison can be done between the results from the PREFUL analysis and the established modalities. Manual segmentation of the lungs takes a long time, so in this study, a smaller number of scans were considered than there were available. In the future, more data should be included and if possible, the segmentation process should be automated.
Nevertheless, PREFUL-MRI has a great diagnostic potential, by eliminating patient discomfort and the need for ionizing radiation, expensive hyper-polarised gases or contrast agents in the assessment of ventilation and perfusion defects in pulmonary diseases. Even in the absence of a very good correlation with other imaging modalities, the results from PREFUL MRI can be used to compare different patients or monitor the progress of the disease in the same patient if the same agreed upon characteristics of the algorithm have been used. Additionally, it opens the possibility of quantifying the ventilation and perfusion and of determining the times-to-peak or the pulmonary wave transit time, which will give a broader view of the patient's health status.

Bibliography

[1] Eric Hoffman and Deokiee Chon. Computed tomography studies of lung ventilation and perfusion. *Proceedings of the American Thoracic Society*, 2:492–8, 506, 2005.

[2] Yuan Lei. *Medical Ventilator System Basics: A clinical guide*. Oxford University Press, 2017.

[3] Grzegorz Bauman, Alexander Scholz, Julien Rivoire, Maxim Terekhov, Janet Friedrich, Andre de Oliveira, Wolfhard Semmler, Laura Maria Schreiber, and Michael Puderbach. Lung ventilation- and perfusion-weighted fourier decomposition magnetic resonance imaging: In vivo validation with hyperpolarized 3he and dynamic contrast-enhanced mri. *Magnetic Resonance in Medicine*, 69(1):229–237, 2013.

[4] Mathieu Lederlin, Grzegorz Bauman, Monika Eichinger, Julien Dinkel, Mathilde Brault, Jürgen Biederer, and Michael Puderbach. Functional mri using fourier decomposition of lung signal: Reproducibility of ventilation- and perfusion-weighted imaging in healthy volunteers. *European Journal of Radiology*, 82(6):1015–1022, 2013.

[5] Grzegorz Bauman, Michael Puderbach, Tobias Heimann, Annette Kopp-Schneider, Eva Fritzsching, Marcus A. Mall, and Monika Eichinger. Validation of fourier decomposition mri with dynamic contrast-enhanced mri using visual and automated scoring of pulmonary perfusion in young cystic fibrosis patients. *European Journal of Radiology*, 82(12):2371–2377, 2013.

[6] Dante P.I. Capaldi, Khadija Sheikh, Fumin Guo, Sarah Svenningsen, Roya Etemad-Rezai, Harvey O. Coxson, Jonathon A. Leipsic, David G. McCormack, and Grace Parraga. Free-breathing pulmonary 1h and hyperpolarized 3he mri: Comparison in copd and bronchiectasis. *Academic Radiology*, 22(3):320–329, 2015.

[7] Till F. Kaireit, Andreas Voskrebenzev, Marcel Gutberlet, Julia Freise, Bertram Jobst, Hans-Ulrich Kauczor, Tobias Welte, Frank Wacker, and Jens Vogel-Claussen. Comparison of quantitative regional perfusion-weighted phase resolved functional lung (preful) mri with dynamic gadolinium-enhanced regional pulmonary perfusion mri in copd patients. *Journal of Magnetic Resonance Imaging*, 49(4):1122–1132, 2019.

[8] Oisin J. O'Connell, Sebastian McWilliams, AnneMarie McGarrigle, Owen J. O'Connor, Fergus Shanahan, David Mullane, Joseph Eustace, Michael M. Maher, and Barry J. Plant. Radiologic imaging in cystic fibrosis: Cumulative effective dose and changing trends over 2 decades. *Chest*, 141(6):1575–1583, 2012.

[9] Grzegorz Bauman, Michael Puderbach, Michael Deimling, Vladimir Jellus, Christophe Chefd'hotel, Julien Dinkel, Christian Hintze, Hans-Ulrich Kauczor, and Lothar R. Schad. Non-contrast-enhanced perfusion and ventilation assessment of the human lung by means of fourier decomposition in proton mri. *Magnetic Resonance in Medicine*, 62(3):656–664, 2009.

[10] Alexander A. Bankier, Carl R. O'Donnell, Vu M. Mai, Pippa Storey, Viviane De Maertelaer, Robert R. Edelman, and Qun Chen. Impact of lung volume on mr signal intensity changes of the lung parenchyma. *Journal of Magnetic Resonance Imaging*, 20(6):961–966, 2004.

[11] Thomas Henzler Gerald Schmid-Bindert Erlend Hodneland Frank G. Zöllner Lothar R. Schad Åsmund Kjørstad, Dominique M. R. Corteville. Quantitative lung ventilation using fourier decomposition mri; comparison and initial study. *Magnetic Resonance Materials in Physics, Biology and Medicine*, 27:467–476, 2014.

[12] Grzegorz Bauman, Ulf Lützen, Mathias Ullrich, Thomas Gaass, Julien Dinkel, Gunnar Elke, Patrick Meybohm, Inéz Frerichs, Beata Hoffmann, Jan Borggrefe, Hans-Christian Knuth, Jasper Schupp, Hermann Prüm, Monika Eichinger, Michael Puderbach, Jürgen Biederer, and Christian Hintze. Pulmonary functional imaging: Qualitative comparison of fourier decomposition mr imaging with spect/ct in porcine lung. *Radiology*, 260(2):551–559, 2011.

[13] Gregor Sommer, Grzegorz Bauman, Marcel Koenigkam-Santos, Christopher Draenkow, Claus Peter Heussel, Hans-Ulrich Kauczor, Heinz-Peter Schlemmer, and Michael Puderbach. Non-contrast-enhanced preoperative assessment of lung perfusion in patients with non-small-cell lung cancer using fourier decomposition magnetic resonance imaging. *European Journal of Radiology*, 82(12):e879–e887, 2013.

[14] Dante P.I. Capaldi, Khadija Sheikh, Rachel L. Eddy, Fumin Guo, Sarah Svenningsen, Parameswaran Nair, David G. McCormack, and Grace Parraga. Free-breathing functional pulmonary mri: Response to bronchodilator and bronchoprovocation in severe asthma. *Academic Radiology*, 24(10):1268–1276, 2017.

[15] Till F. Kaireit, Marcel Gutberlet, Andreas Voskrebenzev, Julia Freise, Tobias Welte, Jens M. Hohlfeld, Frank Wacker, and Jens Vogel-Claussen. Comparison of quantitative regional ventilation-weighted fourier decomposition mri with dynamic fluorinated gas washout mri and lung function testing in copd patients. *Journal of Magnetic Resonance Imaging*, 47(6):1534–1541, 2018.

[16] A. Voskrebenzev, M. Greer, M. Gutberlet, C. Schönfeld, J. Renne, J. Hinrichs, T. Kaireit, T. Welte, F. Wacker, J. Gottlieb, and J. Vogel-Claussen. Detection of chronic lung allograft dysfunction using ventilation-weighted fourier decomposition mri. *American Journal of Transplantation*, 18(8):2050–2060, 2018.

[17] B. Valentin, J. Stabinska, F. Reurik, C. Tell, A.D. Mewes, A. Müller-Lutz, G. Antoch, L.C. Rump, H.J. Wittsack, and A. Ljimani. Feasibility of renal perfusion quantification by fourier decomposition mri. *Magnetic Resonance Imaging*, 85:3–9, 2022.

[18] Åsmund Kjørstad, Dominique M.R. Corteville, Andre Fischer, Thomas Henzler, Gerald Schmid-Bindert, Frank G. Zöllner, and Lothar R. Schad. Quantitative lung perfusion evaluation using fourier decomposition perfusion mri. *Magnetic Resonance in Medicine*, 72(2):558–562, 2014.

[19] Maren Zapke, Hans-Georg Topf, Martin Zenker, Rainer Kuth, Michael Deimling, Peter Kreisler, Manfred Rauh, Bernhard Geiger, and Thomas Rupprecht. Magnetic resonance lung function – a breakthrough for lung imaging and functional assessment? a phantom study and clinical trial. *Respiratory Research*, 7:106, 2006.

[20] Andreas Voskrebenzev, Marcel Gutberlet, Filip Klimeš, Till F. Kaireit, Christian Schönfeld, Alexander Rotärmel, Frank Wacker, and Jens Vogel-Claussen. Feasibility of quantitative regional ventilation and perfusion mapping with phase-resolved functional lung (preful) mri in healthy volunteers and copd, cteph, and cf patients. *Magnetic Resonance in Medicine*, 79(4):2306–2314, 2018.

[21] Lea Behrendt, Andreas Voskrebenzev, Filip Klimeš, Marcel Gutberlet, Hinrich B. Winther, Till F. Kaireit, Tawfik Moher Alsady, Gesa H. Pöhler, Thorsten Derlin, Frank Wacker, and Jens Vogel-Claussen. Validation of automated perfusion-weighted phase-resolved functional lung (preful)-mri in patients with pulmonary diseases. *Journal of Magnetic Resonance Imaging*, 52(1):103–114, 2020.

[22] Till F Kaireit, Agilo Kern, Andreas Voskrebenzev, Gesa H Pöhler, Filip Klimes, Lea Behrendt, Marcel Gutberlet, Tawfik Moher-Alsady, Anna-Maria Dittrich, Frank Wacker, Jens Hohlfeld, and Jens Vogel-Claussen. Flow volume loop and regional ventilation assessment using phase-resolved functional lung (preful) mri: Comparison with 129xenon ventilation mri and lung function testing. *Journal of Magnetic Resonance Imaging*, 53(4):1092–1105, 2021.

[23] Marcus J. Couch, Samal Munidasa, Jonathan H. Rayment, Andreas Voskrebenzev, Ravi Teja Seethamraju, Jens Vogel-Claussen, Felix Ratjen, and Giles Santyr. Comparison of functional free-breathing pulmonary 1h and hyperpolarized 129xe magnetic resonance imaging in pediatric cystic fibrosis. *Academic Radiology*, 28(8):e209–e218, 2021.

[24] Gesa H. Pöhler, Filip Klimeš, Lea Behrendt, Andreas Voskrebenzev, Cristian Crisosto Gonzalez, Frank Wacker, Jens M. Hohlfeld, and Jens Vogel-Claussen. Repeatability of phase-resolved functional lung (preful)-mri ventilation and perfusion parameters in healthy subjects and copd patients. *Journal of Magnetic Resonance Imaging*, 53(3):915–927, 2021.

[25] Tawfik Moher Alsady, Andreas Voskrebenzev, Mark Greer, Lena Becker, Till F. Kaireit, Tobias Welte, Frank Wacker, Jens Gottlieb, and Jens Vogel-Claussen. Mri-derived regional flow-volume loop parameters detect early-stage chronic lung allograft dysfunction. *Journal of Magnetic Resonance Imaging*, 50(6):1873–1882, 2019.

[26] Gesa H. Pöhler, Filip Klimes, Andreas Voskrebenzev, Lea Behrendt, Christoph Czerner, Marcel Gutberlet, Serghei Cebotari, Fabio Ius, Christine Fegbeutel, Christian Schoenfeld, Till F. Kaireit, Erik F. Hauck, Karen M. Olsson, Marius M. Hoeper, Frank Wacker, and Jens Vogel-Claussen. Chronic thromboembolic pulmonary hypertension perioperative monitoring using phase-resolved functional lung (preful)-mri. *Journal of Magnetic Resonance Imaging*, 52(2):610–619, 2020.

[27] Jaber Juntu, Jan Sijbers, Dirk Van Dyck, and Jan Gielen. Bias field correction for mri images. In Marek Kurzyński, Edward Puchała, Michał Woźniak, and Andrzej żołnierek, editors, *Computer Recognition Systems*, pages 543–551. Springer Berlin Heidelberg, 2005.

[28] Bradley Lowekamp, David Chen, Luis Ibanez, and Daniel Blezek. The design of simpleitk. *Frontiers in Neuroinformatics*, 7, 2013.

[29] Ziv Yaniv, Bradley C. Lowekamp, Hans J. Johnson, and Richard Beare. Simpleitk image-analysis notebooks: a collaborative environment for education and reproducible research. *Journal of Digital Imaging*, 31(3):290–303, 2017.

[30] Richard Beare, Bradley Lowekamp, and Ziv Yaniv. Image segmentation, registration and characterization in r with simpleitk. *Journal of Statistical Software*, 86(8):1–35, 2018.

[31] Stefan Klein, Marius Staring, Keelin Murphy, Max A. Viergever, and Josien P. W. Pluim. elastix: A toolbox for intensity-based medical image registration. *IEEE Transactions on Medical Imaging*, 29(1):196–205, 2010.

[32] Denis Shamonin, Esther Bron, Boudewijn Lelieveldt, Marion Smits, Stefan Klein, and Marius Staring. Fast parallel image registration on cpu and gpu for diagnostic classification of alzheimer's disease. *Frontiers in Neuroinformatics*, 7, 2014.

[33] 3d slicer image computing platform.

[34] Kaiming He, Jian Sun, and Xiaoou Tang. Guided image filtering. *IEEE Transactions on Pattern Analysis and Machine Intelligence*, 35(6):1397–1409, 2013.

[35] Julian Glandorf, Filip Klimeš, Lea Behrendt, Andreas Voskrebenzev, Till F. Kaireit, Marcel Gutberlet, Frank Wacker, and Jens Vogel-Claussen. Perfusion quantification using voxel-wise proton density and median signal decay in preful mri. *Magnetic Resonance in Medicine*, 86(3):1482–1493, 2021.

[36] Julian Glandorf, Filip Klimeš, Andreas Voskrebenzev, Marcel Gutberlet, Frank Wacker, and Jens Vogel-Claussen. Effect of intravenously injected gadolinium-based contrast agents on functional lung parameters derived by preful mri. *Magnetic Resonance in Medicine*, 83(3):1045–1054, 2020.

[37] Julian Glandorf, Filip Klimeš, Andreas Voskrebenzev, Marcel Gutberlet, Lea Behrendt, Cristian Crisosto, Frank Wacker, Pierluigi Ciet, Jim M. Wild, and Jens Vogel-Claussen. Comparison of phase-resolved functional lung (preful) mri derived perfusion and ventilation parameters at 1.5t and 3t in healthy volunteers. *PLOS ONE*, 15(12):1–14, 2021.

[38] Filip Klimeš, Andreas Voskrebenzev, Marcel Gutberlet, Agilo Luitger Kern, Lea Behrendt, Robert Grimm, Hendrik Suhling, Cristian Gonzales Crisosto, Till Frederick

Kaireit, Gesa Helen Pöhler, Julian Glandorf, Frank Wacker, and Jens Vogel-Claussen. 3d phase-resolved functional lung ventilation mr imaging in healthy volunteers and patients with chronic pulmonary disease. *Magnetic Resonance in Medicine*, 85(2):912–925, 2021.

[39] Filip Klimeš, Andreas Voskrebenzev, Marcel Gutberlet, Arnd J. Obert, Gesa H. Pöhler, Robert Grimm, Lea Behrendt, Cristian Crisosto, Julian Glandorf, Tawfik Moher Alsady, Frank Wacker, and Jens Vogel-Claussen. Repeatability of dynamic 3d phase-resolved functional lung (preful) ventilation mr imaging in patients with chronic obstructive pulmonary disease and healthy volunteers. *Journal of Magnetic Resonance Imaging*, 54(2):618–629, 2021.

[40] intrasense.fr.